2-2 Atom Optics and Atom Lithography

OHMUKAI Ryuzo and WATANABE Masayoshi

High-resolution atomic channeling using velocity-selected atoms may be able to overcome precision limitations of the conventional atom lithography. We have experimentally clarified the dependence of line width and contrast of atomic patterns in the channeling region on the velocity spread of the atomic source for the first time. Thermal or velocity-selected atomic beams prepared with a one-dimensional magneto-optical trap were employed as the atomic sources. We can show that narrower line width and higher contrast atomic patterns are obtained as the velocity spread becomes narrower. We also successfully produced periodic ytterbium (Yb) narrow lines on a substrate using a near-resonant laser light and the direct-write atom lithography technique. We clearly observed a grating pattern of Yb atoms fabricated on a substrate with a line separation of approximately 200 nm after examining the surface of the substrate with an atomic force microscopy. This is the first demonstration of nanofabrication using the atom-optical approach with Yb atoms.

Keywords
Atom optics, Atom lithography, Magneto-optical trap, Optical molasses, Channeling

1 Introduction

With the recent development of single-mode tunable laser technologies, research and development is underway on the use of the scattering force and dipole force of light to control the motion of atoms. The techniques involved in these studies have developed into a new field of research referred to as "atom optics," which differs significantly from conventional optics, in which light is controlled with matter. In particular, atom lithography [1]-[4] uses laser light to manipulate velocity-selected atoms to form a desired microstructure as these atoms are deposited on a substrate. This technology has enabled high-precision, non-contact generation of fine periodic atomic patterns on the scale of the wavelength of light. This method has drawn a great deal of attention as a new means of nanofabrication, one that differs fundamentally from conventional lithography techniques. This method holds significant potential as new material processing technology applicable to the development of future info-communications devices, including three-dimensional photonic crystals. However, present atom lithography experiments have revealed limitations in the species of atoms that may be used and in the contrast of atomic patterns; these problems must be overcome prior to practical application of atom lithography.

In an attempt to overcome the limitations of conventional atom lithography, we performed experiments using a one-dimensional magneto-optical trap (1D-MOT) [5] to guide and deflect the atomic beam - a fundamental technology for controlling atom source that is indispensable in high-performance atom lithography. With the velocity-selected beam thus obtained, we were able to achieve high-resolution atomic channeling [6]. Further, we conducted the first experiments to date in atom lithography using ytterbium (Yb) atoms, successfully producing intended atomic patterns [7]. This paper reports on the results of

these experiments.

2 High-resolution atomic channeling

2.1 Experimental principles and setup

To prepare for the atom lithography, we first confined the ^{87}Rb atoms within a region the size of a wavelength of light using the dipole force potential induced by an optical standing wave; the channeling experiment was then conducted within the half-wavelength period of the given light wave [8]. We performed the channeling experiments using atomic beams at various velocity distribution widths. Our goal in this experiment was to clarify the effect of the velocity distribution width of the atomic source on the characteristics of the channeled atomic pattern and to improve its resolution.

When an atom enters the optical standing wave, the light imposes a dipole force on the atom. The direction of the force is determined by the sign of the detuning of the light that generates the optical standing wave, and the magnitude of the force is proportional to the gradient of the light intensity. As the spatial intensity distribution of the optical standing wave features a period corresponding to half the wavelength of the light, this standing wave acts as nanometer-scale arrays of cylindrical lenses to direct and focus the atoms. Thus, when an atomic beam with approximately uniform spatial distribution passes through the optical standing wave, the atoms are focused and channeled to the nodes or the antinodes of the standing wave corresponding to half of the period of the light wave.

Figure 1 shows the experimental setup. The apparatus consists of three component sections. The first section generates the atomic beam. In this experiment we used a rubidium (Rb) beam; the goal was therefore to channel ^{85}Rb, using the transition $5S_{1/2}$ F=3→$5P_{3/2}$ F=4. A thermal Rb atomic beam generated using an oven and two pinholes served as the atomic source. The divergence angle of the beam was 10 mrad.

The second section of the apparatus performs velocity selection. The velocity selector employed uses a one-dimensional magneto-optical trap (1D-MOT). This velocity selector performs simultaneous transverse cooling (collimation) and velocity selection of the atomic beam. This configuration represents the first reported use of a 1D-MOT scheme for the atomic beam guide and velocity selector. The 1D-MOT (interaction length 15 cm) is tilted at an angle θ relative to the axis of the thermal atomic beam and is constructed of four copper rods, four rectangular mirrors, and two laser beams.

Two external-cavity diode lasers serve as light sources: one is used to deflect the atomic beam and the other is for repumping atoms, with intensities of 10 mW/cm^2 and 1 mW/cm^2, respectively. These two laser beams are shaped to 15 mm × 3 mm, superposed, set to σ^+-polarization, and introduced into the 1D-MOT. The laser light is multi-reflected from the four rectangular mirrors, as shown in Fig.1. The σ^+-polarized light beam and the σ^--polarized light beam are irradiated to the atomic beam from opposite directions. The four copper rods are placed parallel to the deflection axis and spaced 1.0 cm apart. Electric currents are passed through each of these adjacent rods in alternating directions, generating the quadrupole magnetic field.

As the atoms entering the 1D-MOT region experience strong restoring and damping forces toward the 1D-MOT axis, this tilted axis becomes the deflection axis. As a result, this apparatus can guide atoms within a wide velocity range along this deflection axis, change their directions of propagation, and extract them as a deflected beam. This method can involve the use of transverse laser cooling to collimate the deflected beam sufficiently along the deflection axis while at the same time compressing the beam diameter. This is expected to increase the atomic density of the deflected beam. Further, precise control of the laser frequency enables isotope selection within the extracted atomic beam.

The third part is the channeling section. A

Ti:sapphire laser beam is focused to 1 mm with a lens, reflected by a mirror, and allowed to interact with the atomic beam to generate the optical standing wave that will be used to channel the atoms. To generate the standing wave, the laser light is detuned to +200 MHz; optical power is set to 50 mW. Channeling properties are measured from the frequency shifts of atomic absorption by the channeled Rb atoms. The absorption frequency of an atom at a position x in a strong optical standing wave shows a shift from the resonant frequency (ν_0) without the optical standing wave, which is expressed as the following equation [8]:

$$\nu(x) = \nu_0 - \delta \cdot \left\{ \sqrt{1 + \frac{\Omega(x)^2}{\delta^2}} - 1 \right\}$$

Here, δ is the detuning of the light and $\Omega(x)$ is the Rabi frequency at position x, which is proportional to the intensity of the optical standing wave. In other words, the position of the atom in the optical standing wave can be probed through the frequency shifts of the absorption lines of the atom, and the atomic density at this position can be obtained from the absorption intensity. Scanning the frequency, the probe beam for the frequency shift measurement is introduced through the channeling region, approximately perpendicular to the atomic beam. The beam diameter of the probe beam is set to 1 mm or less. The photodiode receives the transmitted light to measure the atomic absorption.

2.2 Experimental results

First, we will present the results of velocity selection using the 1D-MOT. The resonant laser light was irradiated perpendicular to the atomic beam 35 cm downstream from the 1D-MOT, and the spatial density distribution of the deflected atoms was then obtained from the spatial intensity distribution of the laser-induced fluorescence. Figures 2 (a) - (c) show the results for the deflection angles (θ) of 4, 3, and 1.5 degrees, respectively. Two fluorescence spots were observed in the CCD camera images in all cases. The upper spots were generated by atoms at high velocities propagating in a straight line, with little interaction with the 1D-MOT. The lower spots were generated by the deflected atomic beam. The measured deflection displacement agreed with values calculated from the deflection angle and the flight distance. Similar experiments were conducted at various probe-beam frequencies, with results indicating that the deflected beam consists only of ^{85}Rb atoms.

The velocity distribution of the deflected atomic beam guided by the 1D-MOT was

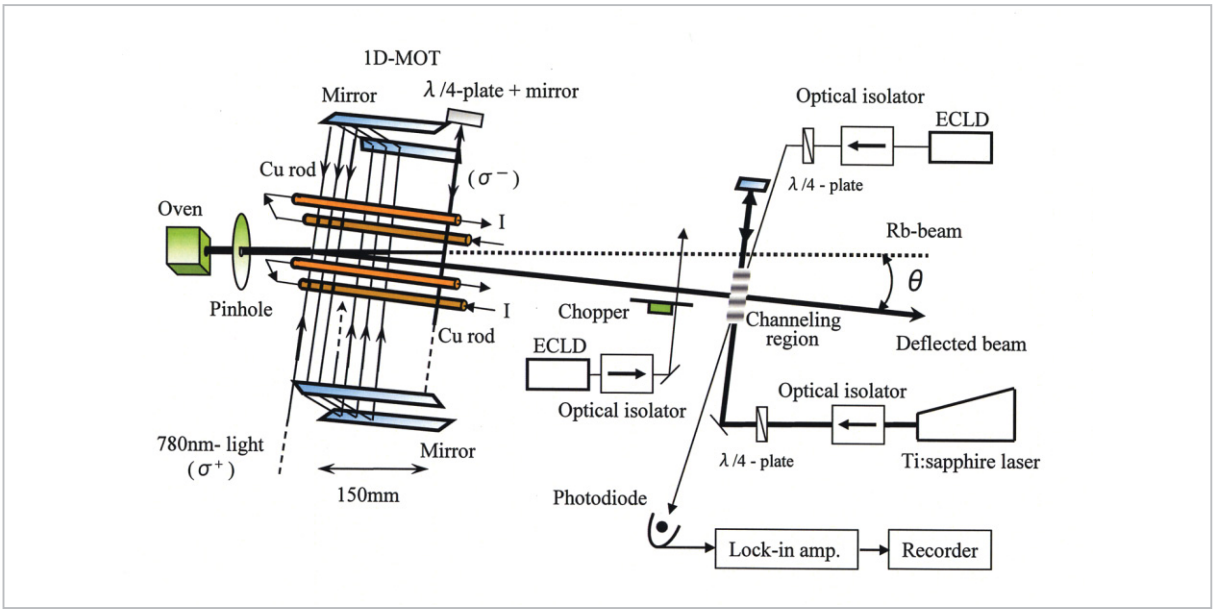

Fig. 1 Experimental configuration for high-resolution atomic channeling

measured, revealing that as the deflection angle is reduced, the upper limit velocity of atoms that can be guided along the deflection axis increases, along with an increase in the density of deflected atoms. For θ = 4°, only atoms with velocities of approximately 120 m/s or less were guided along the deflection axis. At θ = 3°, the deflected beam consisted of atoms with velocities of 180 m/s or less. When the angle was reduced to θ = 1.5°, the upper limit velocity increased to 250 m/s, with deflection efficiency also increasing, to 40 %.

An atomic beam with a smaller θ value features a lower velocity component perpendicular to the deflection axis, and longer interaction time. This is considered to increase the upper limit velocity and the deflection efficiency of the atoms successfully guided. It should be noted that Fig. 2 indicates that the deflected beam was collimated along the deflection axis as intended; the divergence of the deflected beam was 1.5 mrad. The diameter of the deflected beam was also measured and revealed to be smaller than that of the thermal atomic beam in all cases. For θ = 3°, the diameter of the deflected beam was 2 mm, while that of the thermal beam was 8 mm. Thus, the extracted beam simultaneously underwent deflection, collimation, and compression to form a high-density atomic beam. The high collimation and high density of the resultant atomic beam renders this beam suitable as an atomic source in atom lithography.

Next, channeling experiments were performed using the deflected and velocity-selected beam obtained via the method described above as the atomic source. First, the thermal atomic beam, which features the largest velocity spread, was used for channeling; the characteristics of the resultant channeling patterns were then measured. The Rb thermal atomic beam featured a velocity distribution width corresponding to 270 m/s. Figure 3 (a) shows the measured absorption spectrum for the channeling atoms.

As this experiment did not require velocity selection, one-dimensional optical molasses was used to collimate an atom beam with a

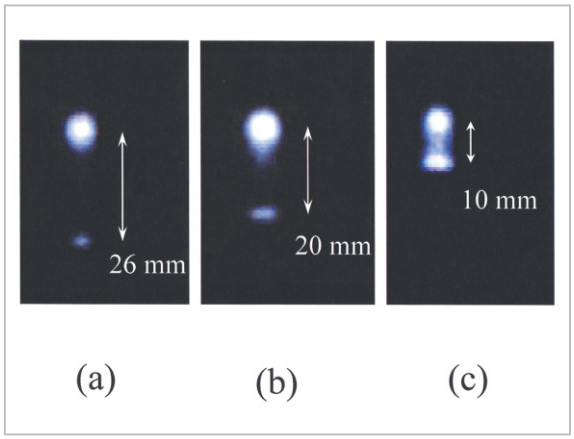

Fig.2 *Results of deflected beam measurement*

divergence angle of 1 mrad, instead of the 1D-MOT. A broad absorption spectrum can be seen in Fig.3 (a). This spectrum differs markedly from the Doppler-free absorption spectrum. Absorption intensities with no frequency shift correspond to atoms in the nodes of the optical standing wave, while absorptions with a larger frequency shift correspond to atoms closer to the antinodes of the optical standing wave. The absorption at a frequency of -120 MHz corresponds to the atoms in the antinodes.

Figure 4 (a) shows the spatial density distribution of the channeled atoms deduced from the frequency shift and absorption intensity. These results show that a grating pattern with a line width (full width at half intensity maximum, or "FWHM") of 100 nm was successfully formed. The contrast of the pattern was approximately 2.6, and the pattern showed a background atomic layer, probably due to absorption by atoms in the probing region with little or no channeling. Figures 3 (b) and (c) show the results of similar experiments using atomic sources with narrower velocity distribution widths. The atomic sources consisted of the deflected beams obtained when the deflection angles (θ) of the 1D-MOT were 1.5 and 3 degrees, respectively, and the corresponding velocity distribution widths of the atomic sources were 100 m/s and 50 m/s, respectively. When the velocity distribution width was smaller and closer to a mono-velocity beam, the absorption increased in the

regions of low frequency shift, while a decreasing absorption intensity gradient became conspicuous toward the regions of larger frequency shift.

Figures 4 (b) and (c) show the spatial density distribution of the atoms during channeling, obtained from the spectra of Fig.3 (b) and (c), respectively. The distributions of the ^{85}Rb atoms in the optical standing wave are steeper than that shown in Fig.4 (a). In Figure 4 (b), a pattern with a line width of 83 nm is observed, and in Fig.4 (c), the line width is even narrower, at 57 nm. This line width value (resolution) is finer than the resolution achieved in conventional optical lithography technology (100 nm). At the same time, pattern contrast is improved, to 3.0 (Fig.4 (b)) and 3.5 (Fig.4 (c)), respectively. These results offer the first experimental evidence for the effects of velocity distribution of the atomic source on channeling characteristics, clarifying that a narrower velocity distribution width in the atomic source leads to higher resolution in atomic channeling. It is clear that high-resolution atomic patterning (atomic lithography) will require high-precision atomic manipulation, and we believe that the foregoing results will prove quite useful in establishing such a technique.

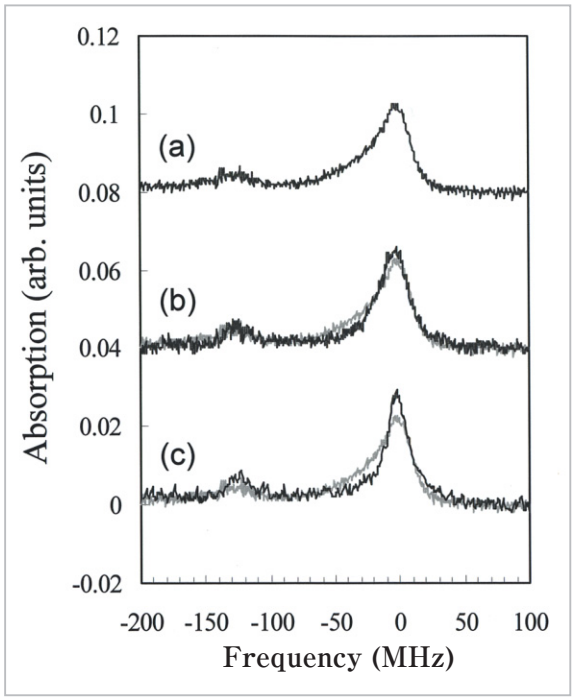

Fig.3 *Absorption spectra of channeling atoms; spectrum for (a) is superposed on (b) and (c) for comparison*

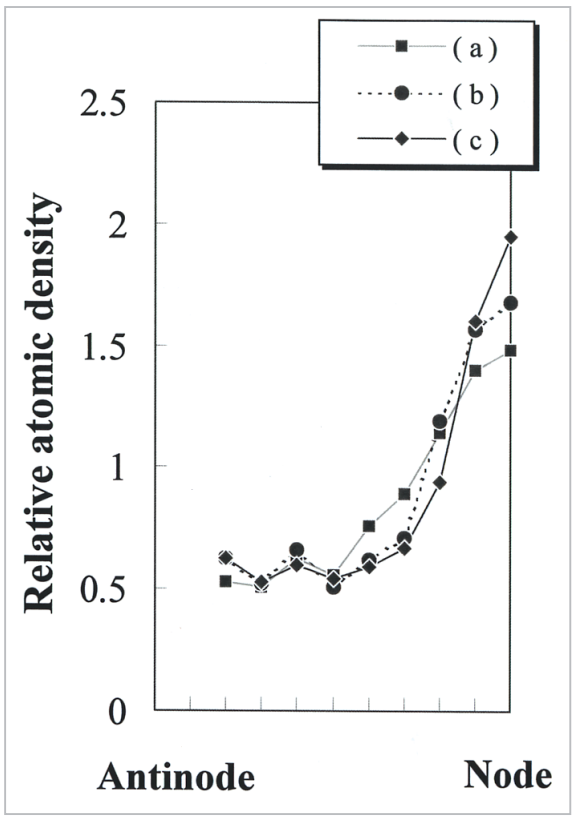

Fig.4 *Channeling pattern results*

3 Atom lithography using ytterbium atoms

3.1 Experimental principles and setup

Based on the technique developed as discussed above, we then proceeded to perform experiments to construct microstructures on the substrate through deposition of the channeled atoms. We chose ytterbium (Yb) as the target atom, which had never been used in atom lithography experiments. High-density Yb thermal atomic beams can be obtained at relatively low temperatures (approximately 800 K), and structures constructed with Yb are stable outside of the vacuum chamber (i.e., exposed to air). The laser wavelength for manipulating Yb atoms is 399 nm, which can be generated using commercially available laser sources. Further, Yb is one of a few atomic species with which Bose-Einstein con-

densation of atomic gas is achieved [9]. This element also has potential in the development of lithographic holography technology using an atom laser. Together these characteristics make this element an extremely significant experimental target.

Figure 5 shows the experimental configuration. A frequency-doubled Ti:sapphire laser, pumped by an Ar-ion laser, was chosen as the light source, providing single-mode (spectral line width of 1 MHz or less) 399-nm light with an output power of 40 mW. Two sets of these laser light sources were used: one for collimation of the atomic beam, and the other for atomic channeling. A thermal atomic beam was generated from an Yb atomic beam with a divergence of 4 mrad, using an oven and two pinholes. An Yb thermal atomic beam consists of 7 isotopes, and in this experiment, the dominant isotope, ^{174}Yb, served as the target of fabrication. The oven temperature was maintained at 800 K during deposition (approximately 30 minutes), and the degree of vacuum in the vacuum chamber was maintained at 1.0×10^{-9} Torr. The generated Yb thermal atomic beam was collimated with the one-dimensional optical molasses to a divergence angle of 1.5 mrad, and this collimated beam was then used as the atomic source for atomic patterning.

The 399-nm light used for the optical molasses was adjusted to an intensity of 45 mW/cm^2 and an interaction length of 15 mm. The laser frequency was detuned by −30 MHz from the resonant frequency of ^{174}Yb, and then stabilized with the temperature-stabilized reference cavity. The collimated beam was then channeled into the optical standing wave. The intensity of this optical standing wave was 40 W/cm^2, and the beam diameter was 0.5 mm. The standing wave was generated by using the method described in Section **2.1**, through reflection of the 399-nm light by a mirror; the frequency detuning was +1.5 GHz.

The silicon substrate was placed directly after the optical standing wave for deposition of the channeled Yb atoms. After the atoms were deposited, the substrate was removed from the vacuum chamber for investigating the characteristics of the resultant surface structures with an atomic force microscope (AFM).

3.2 Experimental results and discussion

Figure 6 shows the results of the Yb atom lithography experiment. Figure 6 (a) is the

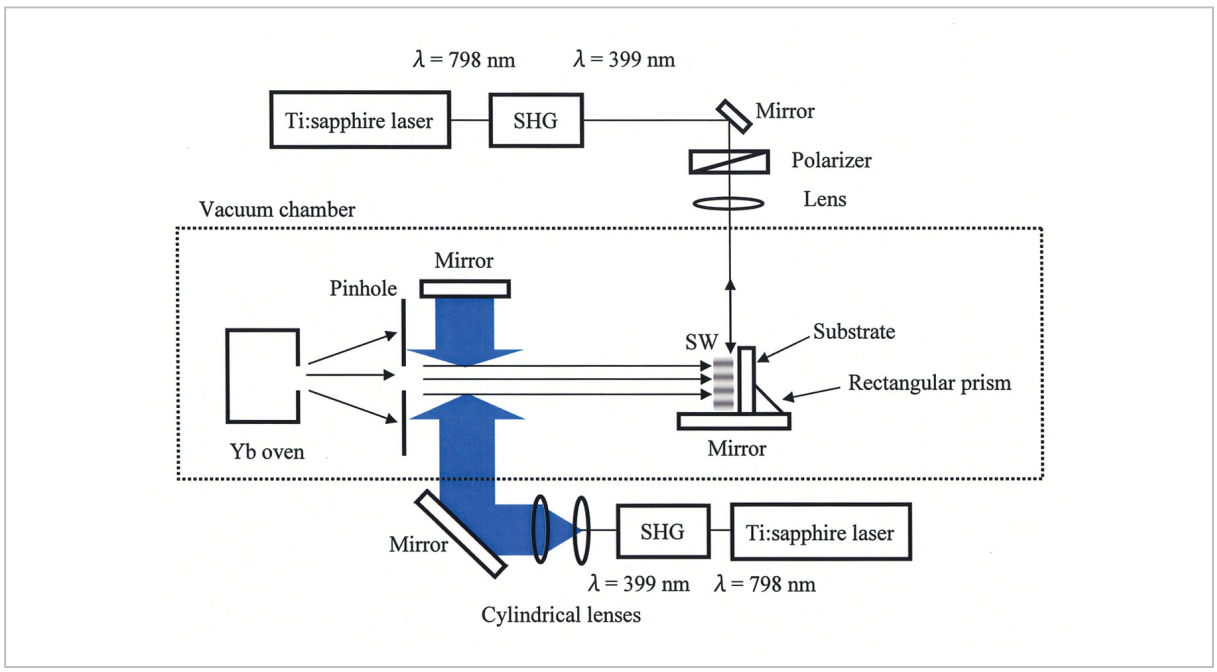

Fig.5 *Experimental configuration for ytterbium atom lithography*

AMF image of the substrate surface with the deposited Yb atoms. The scan range was 10 × 10 micrometers. Color brightness corresponds to the height of the Yb atomic structure. This image shows that a regular and highly-parallel Yb atomic wire structure was successfully formed. The heights and widths of the wires were also uniform. The period of the Yb structure was estimated to be 200 nm, which approximately agrees with the intensity period of the optical standing wave (199.5 nm) used in atomic channeling. Figure 6 (b) shows the typical height distribution of the Yb structure in the range of 3 micrometers. Analysis of the height distribution results reveals that the period of the wire structure is 205 ±9 nm. This value agrees with the value estimated above (199.5 nm) within an acceptable margin of error. The height of the structure is approximately 10 nm, and the line width (FWHM) is 93 ±5 nm. The period and the shape of the pattern agree with the predicted results. These actual results lead to the conclusion that successful manipulation of atoms enabled the fabrication of the intended Yb atomic pattern.

Next, we simulated the Yb atomic channeling process to analyze the line width (approximately 93 nm) obtained in the experiment. For simplicity, the intensity distribution of the optical standing wave is assumed uniformity along the direction of atomic propagation, and also assumed that it can be described along the axis (in the *x* direction) of the optical standing wave with the following equation:

$$I = I_0 \cdot \sin^2(2\pi \cdot x/\lambda)$$

Here, λ is the wavelength of the light used for the optical standing wave and I_0 is the intensity of the light at the antinodes of the optical standing wave. Taking the atomic velocity, the incident position, and the divergence angle as parameters, the channeling processes were calculated for approximately 400,000 atoms to obtain the expected Yb atomic pattern. Figure 7 shows the calculation results. Figure 7 (a) shows the results obtained under the experimental conditions described above. The horizontal axis represents displacement from a node of the optical standing wave, and the vertical axis represents the height of the generated structure. Even under the experimental conditions, an Yb pattern is expected with a line width of 56 nm. The difference between the calculated and the measured value (approximately 40 nm) is probably attributable to factors such as the diffusion of Yb atoms on the substrate, jitter in the intensity and frequency of the optical standing wave, and vibration of the substrate. The actual line width of 56 nm may have been due to imperfect collimation and the velocity distribution of the Yb thermal atomic beam, and the shape

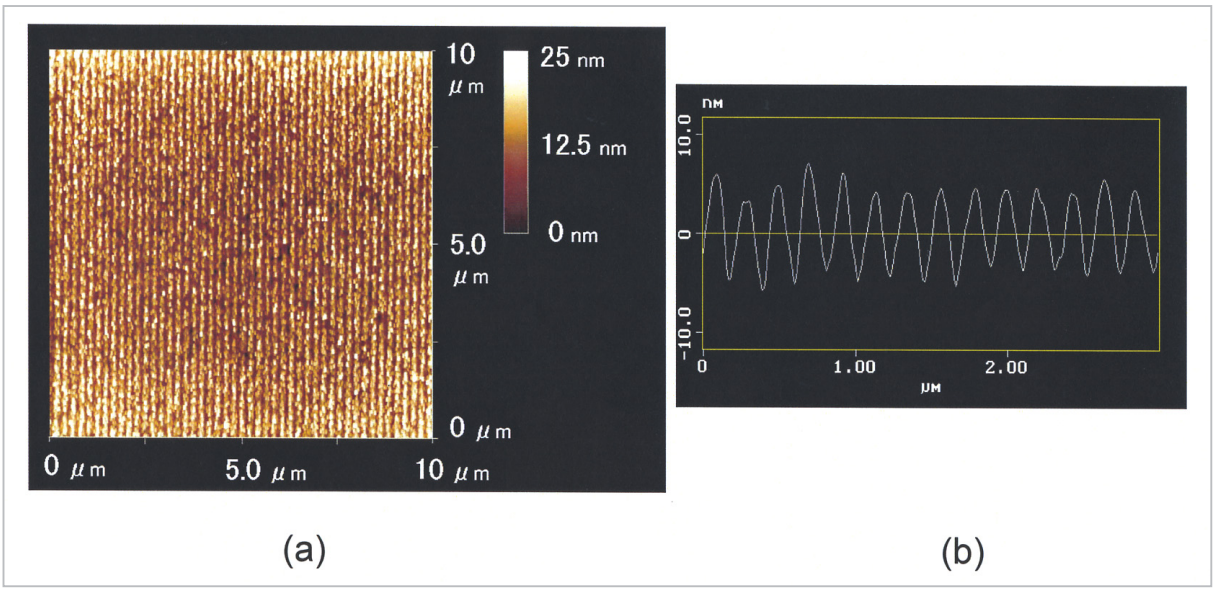

Fig.6 *Experimental results for ytterbium atom lithography*

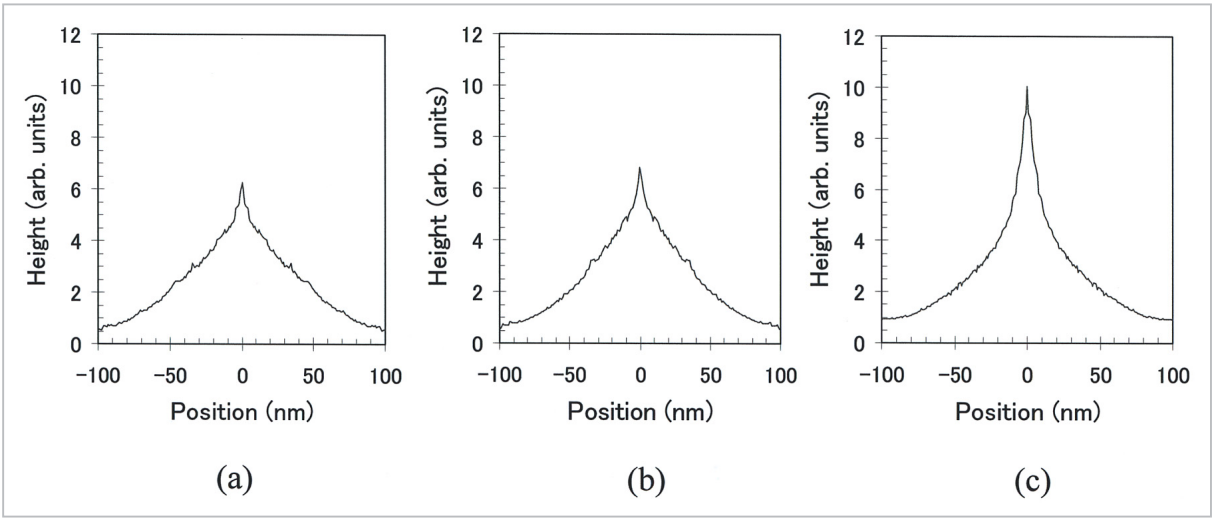

Fig.7 *Simulated results of the ytterbium atomic channeling pattern*

of the dipole potential of the optical standing wave (i.e., deviation from the harmonic potential).

To determine the factors that must be improved to narrow pattern line width significantly, as well as the extent to which it can be narrowed, we continued our calculations with the collimation of the atomic beam as the parameter. Figure 7 (b) shows the Yb atomic pattern calculated with an atomic beam divergence angle of 1.1 mrad. This pattern clearly indicates that an improvement in atomic beam divergence reduces the channeling line width to 42 nm, 14 nm narrower than before the improvement in collimation. This divergence angle (1.1 mrad) corresponds to the Doppler cooling limit of the Yb transition resonating at a wavelength of 399 nm. We believe that this divergence angle can be achieved by increasing the laser intensity of the one-dimensional optical molasses shown in Fig.5. The Yb atomic pattern was calculated assuming that channeling is performed using an atomic beam with further improved divergence (0.2 mrad) as the atomic source. Figure 7 (c) shows the calculated results. The line width of the wire was 20 nm (the narrowest so far), 36 nm narrower than that of Fig.7 (a), representing an approx. 2/3 reduction. These simulation results show that improvement in the collimation of the atomic source can lead to extensive narrowing of line width of the atomic pattern and a corresponding improvement in resolution.

With Yb atoms, an atomic beam with a divergence angle of 0.2 mrad can be obtained using Doppler cooling through the forbidden transition ($^1S_0$ - $^3P_1$) of the Yb atom [10]. One-dimensional optical molasses employing the conventional 399-nm transition and this forbidden transition can thus contribute to experimental applications of the atomic beam.

4 Summary

Guidance and velocity selection of an Rb thermal atomic beam were performed using the 1D-MOT, leading to the first experimental demonstration of high-resolution Rb atomic channeling. Using channeled Yb atoms, a periodic Yb atomic wire structure was successfully constructed on a substrate, in the first demonstration of atom lithography using Yb atoms. The technique developed in this study is not limited to the Rb and Yb used here; in principle it can be applied to atoms such as Cr, Al, and In, which are of significant practical importance in engineering applications. In the future we plan to employ these atoms, as well as mono-velocity atomic beams, in order to promote the development of techniques of atomic patterning offering higher contrast and featuring finer line widths.

References

1 G. Timp, R. E. Behringer, D. M. Tennant, and J. E. Cunningham: Phys. Rev. Lett. 69, 1636, 1992.

2 J. J. McClellant, R. E. Scholten, E. C. Palm, and R. J. Celotta: Science 262, 877, 1993.

3 R. W. McGowan, D. M. Giltner, and S. A. Lee: Opt. Lett. 20, 2535, 1995.

4 U. Dorodofsky, J. Stuhler, Th. Schulze, M. Drewsen, B. Brezger, T. Pfau, and J. Mlynek: Appl. Phys. B 65, 755, 1997.

5 R. Ohmukai, S. Urabe, and M. Watanabe: Appl. Phys. B 69, 123, 1999.

6 R. Ohmukai, S. Urabe, and M. Watanabe: Appl. Phys. B 73, 647, 2001.

7 R. Ohmukai, S. Urabe, and M. Watanabe: Appl. Phys. B 77, 415, 2003.

8 C. Salomon, J. Dalibard, A. Aspect, H. Metcalf, and C. Cohen-Tannoudji: Phys. Rev. Lett. 59, 1659, 1987.

9 Y. Takasu, K. Maki, K. Komori, T. Takano, K. Honda, M. Kumakura, T. Yabuzaki, and Y. Takahashi: Phys. Rev. Lett. 91, 040404, 2003.

10 T. Kuwamoto, K. Honda, Y. Takahashi, and T. Yabuzaki: Phys. Rev. A 60, R745, 1999.

***OHMUKAI Ryuzo**, Ph. D.*

Senior Researcher, Advanced Laser Science Group, Basic and Advanced Research Department

Atom Optics, Quantum Electronics

***WATANABE Masayoshi**, Ph. D.*

Research Center Supervisor, Kansai Advanced Research Center, and Group Leader, Advanced Laser Science Group, Basic and Advanced Research Department

Laser Engineering, Atom Optics